Letters

The spark machining of metallic glasses

A material can be electro-discharge, or spark machined if a spark or arc can be made to jump to the workpiece [1]. Generally however, metallic or near-metallic electrical conductivity is required. Machining occurs by the dispersion of localized molten and/or vaporized regions created by the heat generated in the large potential drop experienced by the avalanching electrons near the anodic workpiece surface [1–5]. These electrons comprise the spark which is initiated by dielectric breakdown across the anode–cathode gap, and is confined by subsequent ionization of a narrow dielectric channel [1, 2]. Numerous models of the dispersion process have been developed, and they fall into three main categories depending on whether the dispersion forces are thermal [1, 6], mechanical [1, 4, 6, 7] or electro-mechanical [8, 9, 10] in origin.

It is thought that for the relatively short pulse (a few nanoseconds in duration) sparks created by the relaxation (RC) circuits of commercial electro-discharge machining units, the limiting erosion crater profile corresponds to a melt isothermal surface [3]. In practice, profiles are modified by forces acting during the discharge which shift material to form either a raised rim at the periphery of the crater or inter-electrode bridges within the crater. However, it would appear that all reported investigations of crater profiles have considered solid materials with first order, discontinuous viscosity changes at their melting points. Hence liquid flow predominates because over the short loading times involved, solid flow is negligible even in the most ductile conductors such as indium. If material flow can occur below the melting point, it is anticipated that crater profiles and erosion rates, contrary to reported observations [1, 6, 11], need not correlate with the melting point. This would be the case for a glass which is characterized by a second order structural transition at the glass transition temperature such that viscous deformation can take place at temperatures that are well below the melting point of the corresponding crystalline material. It would therefore be of interest to examine erosion crater profiles produced by spark machining metallic glasses.

Ribbons (2 mm wide and 0.015 mm thick) of $Pd_{781}Cu_{55}Si_{164}$ and $Fe_{72}Ni_8P_{13}C_7$ glasses were spark machined using a relaxation type (Servomet, Model SMD) electro-discharge machining unit. Short lengths of the ribbons were rigidly clamped to the anodic worktable and machining was carried out by lowering a cathode under servo control for 5 sec after initiation of the first spark. The cathode comprised a 10 mm in diameter 70/30 brass rod with a flat, polished end face. Machining was conducted in clean circulating kerosene using Range setting number 5, corresponding to a 0.05 μ capacitance with a 180 V gap voltage. Following ultrasonic cleaning in acetone and xylene, the machined workpiece surfaces were examined by scanning microscopy.

In order to compare erosion crater profiles formed on the metallic glass surfaces with those arising on the surfaces of crystalline metals, the following pure (> 99.9%) metals were also spark machined: In, Al, Cu, Fe, Ni and Ta. Care was taken to ensure that the crystalline metals were machined under the same conditions as those employed for the non-crystalline alloys. Unfortunately, fully crystallized specimens of the glasses were extremely brittle and could not be machined without fragmentation. However, some partially crystalline specimens, obtained by isothermally heat treating the glasses, could be machined and erosion craters formed on the surfaces of these specimens were also investigated.

Typical erosion craters observed on the spark-machined surfaces of the Pd- and Fe-based glass ribbons are imaged in Figs. 1a and b respectively. The craters were characterized by (i) the absence of rims of displaced material; (ii) the presence of central columns; and (iii) shearing at the crater peripheries. The height of the column tended to decrease with a decrease in the crater diameter and the inner edges of the crater boundaries tended to be corrugated. Electron microprobe analyses indicated that the tops of the columns were of the same composition as the bulk material. Hence they did not arise from bridging [6] since this would probably have led to the deposition of

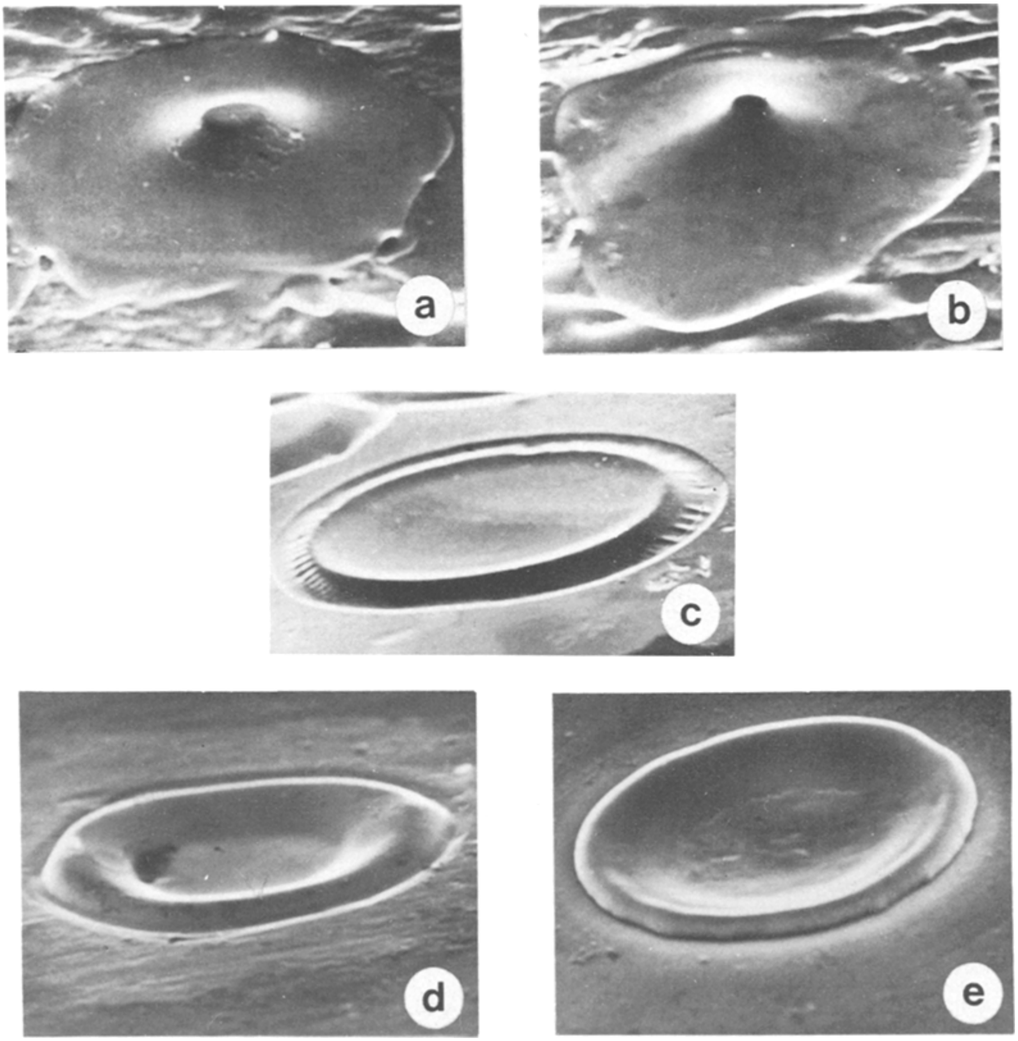

Figure 1 Spark machining erosion craters; (a) $Pd_{781}Cu_{55}Si_{164}$ glass, (b) $Fe_{72}Ni_8P_{13}C_7$ glass, (c) partially crystalline $Pd_{781}Cu_{55}Si_{164}$ alloy (heat treatment: 650 K for 600 sec), (d) Al, (e) Ni. (Magnifications × 2000).

cathode material on the anodic bridge remnants.

Fig. 1c demonstrates the observations that craters formed on the surfaces of partially crystalline specimens were, in most respects, similar to those produced by spark machining the glassy alloys. The most notable difference appeared to be a reduction in the maximum observed height of the central column to the extent that the column was often merely a broad, flat plateau.

Erosion craters, similar to those imaged in Figs. 1d and e for Al and Ni respectively, were observed on the machined surfaces of all the crystalline pure metals investigated. It can be seen that these craters have rims of displaced material, no central columns and no corrugations. Resolidified droplets in and around the craters were not observed, indicating that the primary profile modification mechanism for the crystalline metals, under the existing machining conditions, was the radial flow of liquid metal. These crater profiles were equivalent to those reported for Fe, Cr, Cu and Ta [2]; Mg, In, Al, Fe and Mo [11]; and for V, Nb and Ta [6]. The unusual craters observed on the metallic glass surfaces must therefore have resulted from characteristic workpiece properties and not from the operation of abnormal machining conditions that may have arisen in the present study. It is also reasonable to suppose that the development of the unusual crater profiles was related to the ability of the glassy workpieces to deform viscously at relatively low temperatures. This behaviour was presumably possible because there was insufficient time for the workpieces to crystallize during spark erosion. The observations that central columns arose at the crater centres indicated that the spark machining process produced normal forces which pulled the viscous material in the heated workpiece zone towards the other electrode.

The volume of material that deformed was approximately the same for both the non-crystalline and crystalline specimens in spite of the fact that the former were potentially able to deform viscously at low temperatures. It was therefore likely that the formation of the central columns modified the spark discharge characteristics so as to produce less heating of the glassy workpieces. The same feature probably also suppressed the formation of radial discharge pressures [6, 12, 13] at the surface and the attendant displacement of material to form a rim. It can also be tentatively concluded that in order for a significant amount of spark modification to occur it would have been necessary for the central column to be formed at an early stage of the spark discharge, such as during the pre-arc ignition stage when there is thought to be a strong electrostatic field in the inter-electrode gap [8].

The radial corrugations around the crater edges possibly developed as a result of a Rayleigh–Taylor hydrodynamic instability caused by the rapid acceleration of the interface between two viscous liquids (dielectric and heated glass) in the direction of the denser fluid. The acceleration was brought about by the pulling force that created the central column. Moreover, flow constriction during the displacement of material towards the crater centre would have enhanced the degree of corrugation.

References

1. I. A. BUCKLOW and M. COLE, *Met. Rev.* **14** (1969) 103.
2. H. K. LLOYD and R. H. WARREN, *J. Iron Steel Inst.* **203** (1965) 238.
3. F. S. VAN DIJEK and W. L. DUTRE, *J. Phys. (D)* **7** (1974) 879.
4. E. W. GRAY and J. R. PHARNEY, *J. Appl. Phys.* **45** (1964) 667.
5. J. E. GREENE and J. L. GUERRO-ALVEREZ, *Met. Trans.* **5** (1974) 695.
6. *Idem, Trans. ASME* **95B** (1973) 965.
7. D. W. RUDORFF, *Engineers Digest* **10** (1949) 306.
8. M. M. ATTALA, *Bell Syst. Tech. J.* **34** (1955) 203.
9. J. L. SMITH and W. S. BOYLE, **38** (1959) 537.
10. E. M. WILLIAMS, *Trans. Amer. Inst. Elect. Eng.* **71** (1952) 105.
11. M. M. BRUMA, *Bull. Soc. Franc. Elec.* **1** (1960) 840.
12. H. KURAGUGI, *CIRP* **13** (1966) 313.
13. P. KISLINK, *J. Appl. Phys.* **25** (1954) 897.

Received 14 June
and accepted 25 July 1977.

P. G. BOSWELL
Department of Mining and Metallurgical Engineering, University of Queensland,
St. Lucia, Australia, 4067.

Amorphous thin films of stainless steel

In recent years it has become clear that non-crystalline metals and alloys can exhibit different physical and electro-chemical properties to equivalent or similar crystalline phases [1]. The extent of these differences can be wide because it is possible to prepare single phase, non-crystalline alloys at compositions which are not stable in the crystalline form. In particular, mention can be made of transition metal–"metalloid" alloys, such as $Fe_{40}Ni_{40}P_{14}B_6$ and $Fe_{80}B_{20}$, prepared as ribbons or foils by rapid quenching from the melt, which have very good and potentially useful "soft" magnetic properties [1, 2]. Recent work [1, 3–5] on the electrochemical properties of similar alloys of the general type Fe–Cr–Ni–P–C suggest that increased corrosion resistance can be obtained in the amorphous phase. Such glassy phases can also be obtained in films and coatings deposited from the vapour by thermal evaporation or sputtering. In many cases it is necessary to form the deposited layer onto a substrate cooled below room temperature, typically to liquid nitrogen or liquid helium temperatures. Amorphous alloy films also have novel and specific properties related to their non-crystalline atomic arrangement, microstructure